Biosensors and Bioelectronics 129 (2019) 29–35

Contents lists available at ScienceDirect

Biosensors and Bioelectronics

journal homepage: www.elsevier.com/locate/bios

Integration of a field effect transistor-based aptasensor under a hydrophobic membrane for bioelectronic nose applications

Alexander E. Kuznetsov*, Natalia V. Komarova, Evgeniy V. Kuznetsov, Maria S. Andrianova, Vitaliy P. Grudtsov, Elena N. Rybachek, Kirill V. Puchnin, Dmitriy V. Ryazantsev, Alexander N. Saurov

Scientific-Manufacturing Complex Technological Centre, 1–7 Shokin Square, Zelenograd, 124498 Moscow, Russian Federation

ARTICLE INFO

Keywords:
Bioelectronic nose
ISFET
Aptamer
Hydrophobic surface
Hydrophilic surface
Gas-to-liquid interface
Self-assembled monolayers

ABSTRACT

A new bioelectronic nose based on a field effect transistor coupled with an aptamer as the sensing element was developed. The gas-to-liquid extraction interface required for appropriate aptamer function was integrated into standard CMOS technology. It was developed with the use of a sacrificial aluminium etching technique combined with surface modifications by silanes for wettability control. As a proof of concept, aptamer Van74 for vanillin was immobilized on the sensitive surface of the ISFET. The developed microsystem can selectively detect vanillin vapor in a concentration range from 2.7 ppt to 0.3 ppm, with a detection limit of 2.7 ppt. The sensor was able to detect vanillin in a gas sample obtained from roasted coffee beans. This outcome provides a foundation for developing a new generation of bioelectronic noses for the detection and discrimination of volatile compounds.

1. Introduction

Ambient air is rich in different types of odourous and other notable compounds. Detection and identification of odourants offer a variety of potential applications in different fields of the economy such as the food and cosmetics industry, health diagnostics and environmental monitoring. Conventional methods of identification of selected odourants occurring in air include chromatographic techniques coupled with suitable detectors. These techniques are labourious, bulky and require complicated stages of sample collection with appropriate preparation for analysis, rendering them unavailable for day-to-day use.

On the other hand, one can observe a tendency to implement the"electronic noses" as supplementation to classic analytical techniques in medical diagnostics (Fitzgerald and Fenniri, 2017) and the food industry (Sanaeifar et al., 2017)."Electronic noses" use several sensors with different signal transduction principles and an appropriate pattern recognition system. However, such sensor arrays are still insufficient in their performance compared to established methods of odour analysis in most applications. Their usage is restricted by susceptibility to ambient humidity and temperature, lack of sensitivity and ability to detect only a select few classes of molecules (Göpel, 2000).

In recent years, increasing attention has addressed the development of biosensors for detection and discrimination of specific odourants. The so-called bioelectronic nose (or biomimetic electronic nose), as a type of electronic nose, overcomes the selectivity limitations due to application of biological receptors on the surface of the employed transducers. Different types of biological materials may be used to mimic natural olfactory systems: olfactory epithelium (Liu et al., 2010), olfactory receptor cells (Liu et al., 2006), olfactory receptor proteins (Goldsmith et al., 2011; Wu, 1999), odourant binding proteins (Hou et al., 2005) and short peptides (Lim et al., 2013). The bioelectronic noses based on olfactory epithelium and olfactory receptor cells employ the detection of change in electric potential produced by the cell. In this case, binding between odourant and olfactory receptors leads to activation of ionic transport and depolarization of the cell membrane (Schild and Restrepo, 1998). Because isolation and in vitro culture of the olfactory receptor neuron cells is challenging, cells exhibiting expression of the olfactory receptor proteins are used (Misawa et al., 2010; Vidic et al., 2006). Separate olfactory receptor proteins incorporated within double-layered lipids or odourant binding proteins may be applied as an alternative to cells (Di Pietrantonio et al., 2013; Sung et al., 2006). Anchoring this type of biomaterial on a chip is complicated, and so the possibility of reuse and repeatability is not always provided (Wasilewski et al., 2017).

Another promising approach is to utilize short peptides responsible for binding instead of entire proteins (Lim et al., 2013). However, the identification of specific sites on the olfactory receptor proteins for peptide develop can be labour-consuming, costly and impractical for

* Corresponding author.
E-mail address: kae@tcen.ru (A.E. Kuznetsov).

https://doi.org/10.1016/j.bios.2019.01.013
Received 17 September 2018; Received in revised form 2 January 2019; Accepted 4 January 2019
Available online 15 January 2019
0956-5663/

many types of olfactory receptors (Wasilewski et al., 2018).

In recent years, aptamers have been attracting attention as a prospective new analogue of antibodies. Aptamers are short single-stranded DNA or RNA that may selectively bind to desired targets (Ellington and Szostak, 1990; Tuerk and Gold, 1990). In comparison to the abovementioned cell receptors and peptides, DNA aptamers as receptors require less maintenance and may be easily synthesized when the DNA sequence is established. On the other hand, field effect transistors (FET) are becoming popular in the development of odour sensors (Cave et al., 2019). Biomaterial immobilized on the gate surface allows detection of electrical signals generated due to odourant exposure.

To this point, only a few sensors based on FET and aptamers are known. For example, the binding of a low molecular weight adenosine to its aptamer was monitored with an ion-selective field effect transistor (ISFET). The sensitivity limit of the device is 5×10^{-5} M (Zayats et al., 2006). Aptamer–thrombin affinity binding was also monitored on a single-walled carbon nanotube FET device (So et al., 2005). The detection of platelet-derived growth factor via a solution-gate field-effect transistor has been demonstrated using aptamers immobilized on a diamond surface (Ruslinda et al., 2010). A bifunctional aptamer that includes two aptamer units for cocaine and adenosine 5′-monophosphate was used in combination with a field-effect transistor (Elbaz et al., 2008). ISFET is applied to sense aptamer-cocaine complexes with a detection limit of 1×10^{-6} M (Sharon et al., 2009).

To overcome the drawbacks of existing gas sensors, we report the usage of ISFET coupled with aptamer for bioelectronic nose applications. In our previous work, we have demonstrated that DNA-aptamers to odourous substances may be obtained by implementation of the Capture-SELEX protocol. Moreover, we have shown that the ISFET-based aptasensor may be effectively used to detect vanillin in liquid samples (Kuznetsov et al., 2018). Bioelectronic noses can function appropriately only when the applied bioreceptors are immersed in liquid medium to maintain their activity. For this reason, we insert ISFET in hydrophilic microchannels and fabricate hydrophobic membranes for gas-liquid exchange directly over ISFET using self-assembled monolayers (SAM) modifications and processes compatible with standard CMOS technology. The resulting microsystem with aptasensor under membrane allows direct detection of vanillin from gas samples without additional extraction techniques.

2. Materials and methods

2.1. Reagents and materials

All reagents were purchased from Sigma-Aldrich (Germany) unless otherwise indicated. Carboxyethylsilanetriol sodium salt solution (CEST) was purchased from ABCR GmbH (Germany). The aptamer to vanillin, Van74, was obtained via the Capture-SELEX protocol described in detail in our previous work (Kuznetsov et al., 2018). Van74 was synthetized by Evrogen (Russia). Complementary probe was synthetized by Microsynth AG (Switzerland). Azidobutyric acid N-hydroxysuccinimide and Cu(II)-TBTA complex were supplied by Lumiprobe (Russia).

2.2. Device fabrication

The chip with n-type ISFET was fabricated using standard 1.2 μm FD SOI CMOS technology on 4'-SOI SIMOX wafers (p-type) with a 0.18 μm thick active layer, 0.38 μm thick insulating layer, and 12–22 Ω cm resistivity in SMC "Technological Centre", Russia. The active layer was further thinned to 100 nm by oxidation. After the formation of n- and p-MOS transistors, 50 nm of tantalum was deposited by PVD onto 10 nm SiO_2 gate dielectric, then a standard metallization step was carried out. During the metallization step, TiN layer was formed before Al deposition on tantalum. After that, deposition of $SiO_2/Si_3N_4/SiO_2$ layers occurred. These layers served the functions of both membrane bulk and chip passivation. Membrane pores were formed by plasma etching of $SiO_2/Si_3N_4/SiO_2$ layers using a photoresist mask. After that (Fig. 1S), the wafer surface was modified by immersion in toluene with octyltriethoxysilane (OTS) (OTS:toluene = 1:2000) for 15 min. Wafers were rinsed in toluene and baked at 150 °C for 30 min. Unlike organofluorine silanes that may result in higher values of contact angle but result in poor photoresist adhesion, the OTS-based layer acts similar to a promoter for photoresist deposition, which is necessary for subsequent etching.

To form capillary microchannels, a sacrificial aluminium etching (SALE) technique was used (Westberg et al., 1996). To this end, a pattern corresponding to capillaries was included in the photomask at the standard CMOS metallization stage. Standard electrical pads were protected by photoresist, and sacrificial Al was etched by 28% hydrochloric acid. Wafers were then rinsed in DI water and dried by N_2.

After Al etching, wafers were immersed in 1% CEST in DI water for 120 min, rinsed, and baked at 110 °C for 60 min. Ammonium peroxide solution (37% NH_4OH: 32% H_2O_2 = 1:1) was used to remove TiN from the Ta gate of the ISFET in capillary channels. Due to the ammonium peroxide solution, a Ta_2O_5 layer was also grown atop the Ta during this operation, forming a floating gate of ISFET. At the end of TiN etching, the protective photoresist was removed by standard operations. Aptamer immobilization was applied to the Ta_2O_5 sensor sensitive surface after wafer cutting.

2.3. Aptamer immobilization

Chips with ISFETs were immersed in 3% 3-aminopropyltriethoxysilane in methanol for 45 min and washed with ethanol after surface modification. Then, the surface was activated for Cu-catalysed click chemistry by reaction with 4 mM azidobutyric-N-hydroxysuccinimide solution in 20 mM Tris-HCl, pH 8.4 for 2 h. The alkyne-modified aptamer was"clicked" onto the transistor sensitive surface by the azide-alkyne cycloaddition reaction during overnight incubation with 1 μM aptamer, 50 μM Cu(II)-TBTA and 2 mM ascorbic acid solution in 20 mM Tris-HCl, pH 8.4. After aptamer immobilization, the aptamer was hybridized with a short complementary probe (5'-Bio-GTC-Spacer18-CATCGAGACTCC-3') during incubation with 20 pM probe solution in selection buffer [100 mM NaCl, 20 mM Tris-HCl, pH 7.6, 2 mM $MgCl_2$, 5 mM KCl, 1 mM $CaCl_2$] for 2 h.

2.4. Electrochemical measurements

ISFET I-V curves (showing dependence of the drain current I_D on the reference electrode voltage V_G) were recorded using an Agilent B1500A semiconductor device parameter analyzer (USA) and Cascade PM5 probe station (USA) with Agilent VEE Pro, as described previously (Andrianova et al., 2016). As a biosensor, the ISFET was used in subthreshold mode. The operating mode was determined from the I_D-V_G curves (derived at the drain voltage V_D = 0.1 V). Time-dependent changes in the current I_D (V_G = constant) were recorded. For data processing, surface potential calculations ($\Delta I_D \rightarrow \Delta\varphi$) were made. For each experiment, 2–3 baseline measurements in buffer solution for ISFET stabilization were performed before sample injection. Signal from sample was calculated as the absolute value of the difference between baseline and sample after ~300 s of sample addition.

All measurements were repeated three times with different chips, and standard deviations were calculated.

2.5. Target sample preparation

100 μL of target compound solution with specified concentration were placed in 15 mL tubes. The tubes were sealed with Parafilm and heated for 1 h at 80 °C in a thermostat (Eppendorf, Germany). A probe of 1 mL of the air from each tube was sampled by a syringe. Concentration of vapor vanillin was calculated using the Antoine

equation at 82 °C (Carl, 2015). Green beans of robusta coffee purchased in the local market were employed for matrix effect study. 5 g of green beans were drenched with 100 µL of 65 µM vanillin solution and roasted at 100 °C for 10 min.

2.6. Study of surface modifications

The p-type silicon boron-doped wafer was cut to prepare test slides (4 × 4 mm). These slides were used to ensure the stability of silanes monolayers during microsystem fabrication.

Slides with formed monolayers (OTS and CEST) passed through the same steps as used for microsystem fabrication. The films were characterized by contact angle studies after each process step. Water wetting contact angle measurements were conducted at room temperature (20 °C) using an OCA 15EC DataPhysics Instrument (Germany). Deionized water (electrical resistance = 18.2 MΩ cm) was dropped onto each surface, and the contact angles were assessed using SCA 20 software. Terminal values of the contact angles were taken as an average of three measurements on different parts of each sample.

To control DNA immobilization on the modified surfaces glucose oxidase-horse radish peroxidase (GOX-HRP) assay was performed. For this purpose, after DNA immobilization slides were hybridized with complementary biotin containing probe and incubated with streptavidin-GOX conjugate solution (20 µg/mL) in SB for 1.5 h.

GOX enzyme activity was measured spectrophotometrically in buffer solution (100 mM citrate-phosphate buffer, pH 5.08), containing TMB solution (300 µM), HRP solution (6×10^{-8} M) and glucose solution (1.2 mM) using Tecan Infinite M200 microplate reader (Austria). Enzyme activity and initial reaction rate were detected based on accumulation of colored reaction product at λ = 650 nm (Khosravi et al., 2012).

3. Results and discussion

3.1. Device design

A new concept of gas-to-liquid extraction interface as an essential part of bioelectronic nose was developed. This concept implies the ISFET which is placed under the hydrophobic membrane in the hydrophilic chamber with capillaries on the silicon chip (Fig. 1).

Surface modifications by silanes enable employment of the capillary effect to fill the picovolume cavity under the membrane during the following experiments. The hydrophobic layer created on the walls of membrane pores prevents the buffer solution from escaping the cavity under the membrane while at the same time allowing chemical compounds from the gaseous phase to pass through.

Microfluidics can be built on top of IC substrates using SALE micromachining technique which is fully IC-compatible (Westberg et al., 1996). Fabrication of gas-to-liquid interface on the chip consisted of four main stages: deposition of a hydrophobic layer onto the SiO_2 membrane and pore walls, removal of aluminium sacrificial layer by SALE technique, creation of a hydrophilic layer on the walls of the resulting cavity and etching of TiN mask under the formed membrane for access to the ISFET sensitive surface. The resulting structures formed on a chip are presented in Fig. 1A. Separated ISFETs were encapsulated under the membrane with pore size of 2 × 2 µm in a 10 pL volume chamber with dimensions of 94 × 114 × 1 µm (Fig. 1B).

Surface hydrophobization and hydrophilization were achieved by its modification with appropriate silanes: OTS and CEST, respectively. After deposition from liquid phase, OTS forms a hydrophobic layer on the oxide surface with contact angle of 75–85° (Supp. Fig. 1S). This angle decreased to ~70 degrees after photoresist removal and stayed the same after TiN etching in NH_4OH:H_2O_2 and conducting of click-chemistry reactions used for aptamer immobilization. It indicates that OTS film remains stable during bioelectronic nose fabrication. Modification of the inner walls formed after aluminium etching with CEST resulted in a stable hydrophilic surface (5–10 degree contact angle) (Supp. Fig. 1S). The wetting contact angle of CEST films after aptamer immobilization also remained the same providing stable surface for capillary effect.

On the final step of the bioelectronic nose fabrication ammonium peroxide solution was used to selectively remove TiN from the Ta gate of the ISFET which protects sensitive surface from OTS and CEST film formation. This enables covalent immobilization of DNA via aminosilane on the prepared Ta_2O_5 sensitive surface (Supp. Fig. 2S).

Additional studies of test slides using glucose oxidase-horse radish peroxidase assay revealed that DNA immobilization via click-chemistry does not pass if the surface of silicon oxide is modified with CEST and OTS (Supp. Fig. 3S). However, surface functionalization flow implies incubation of CEST and OTS surfaces with APTES solution. Measurement of activity showed that in this case partial immobilization of DNA on these surfaces occurred. This can be associated with the formation of mixed films: due to incomplete uniformity of the SAM, as well as the formation of a bond between the aminosilane and the partly hydrolyzed anchoring silane groups of CEST and OTS. Comparison of activities of the test slides showed that the aptamer was mostly immobilized on the sensitive surface than on the microfluidic walls and pores (Supp. Fig. 4S). Incorporation of three types of silanes with different functional groups in fabrication process allows us to immobilize DNA-aptamers mostly on Ta_2O_5 surface and to minimize DNA adsorption on non-sensitive microsystem surface.

3.1.1. ISFET characterization

Measurements were carried out on ISFET with 560 µm channel width (W), 12 µm channel length (L), and sensitive surface area 556 × 54 μm^2, located directly in the microfluidic channel beneath a 94 × 114 μm^2 membrane (Fig. 2). Because of higher W/L ratio, this configuration allows for higher drain currents and wider subthreshold mode, which is the region where the measurements are made. It also utilizes most of the area under the membrane as sensitive surface of the transistor, which is then used for aptamer immobilization. During experiments, the contact to ISFET gate was made through buffer via capillary microchannels, while reference voltage was provided by Pt electrode. This system maintained the constant immersion of the ISFET sensitive surface in the buffer while maintaining contact with the external environment through the hydrophobic membrane.

Current-voltage characteristics of developed ISFETs were studied. I_D-V_G curves of the fabricated ISFET were reproducible and no significant hysteresis (0.76 +/− 0.05 mV) was observed. The average value of the subthreshold swing was 71.5 + /− 4.8 mV/dec (Fig. 3).

3.2. Detection of vanillin vapor

Vanillin (4-hydroxy-3-methoxybenzaldehyde) is one of the most popular flavouring agents used in beverages, baked goods, chocolates, and other sweet foods. In our previous work, we obtained and characterized the Van74 DNA aptamer with affinity to this odourant molecule. In this work, we used Van74 and vanillin as a model system to study the developed microsystem with ISFET under hydrophobic membrane.

The hydrophobic surface of the chip permits us to use a droplet to fill the microfluidic system under the membrane. The droplet volume was kept constant by syringe pump. For ISFET operation, the reference electrode was immersed in the droplet (Fig. 1A). After gas injection, target molecules diffused through the pores to the chamber under the membrane and were captured by aptamer molecules on the ISFET sensitive surface.

Fig. 4 shows real time response of the modified ISFETs. An increase in vanillin concentration leads to an increase in response. In the employed detection scheme, vanillin replaced the hybridized probe on the sensitive surface resulting in decrease of negative charge near the sensitive surface. Negative charge decrease leads to surface potential

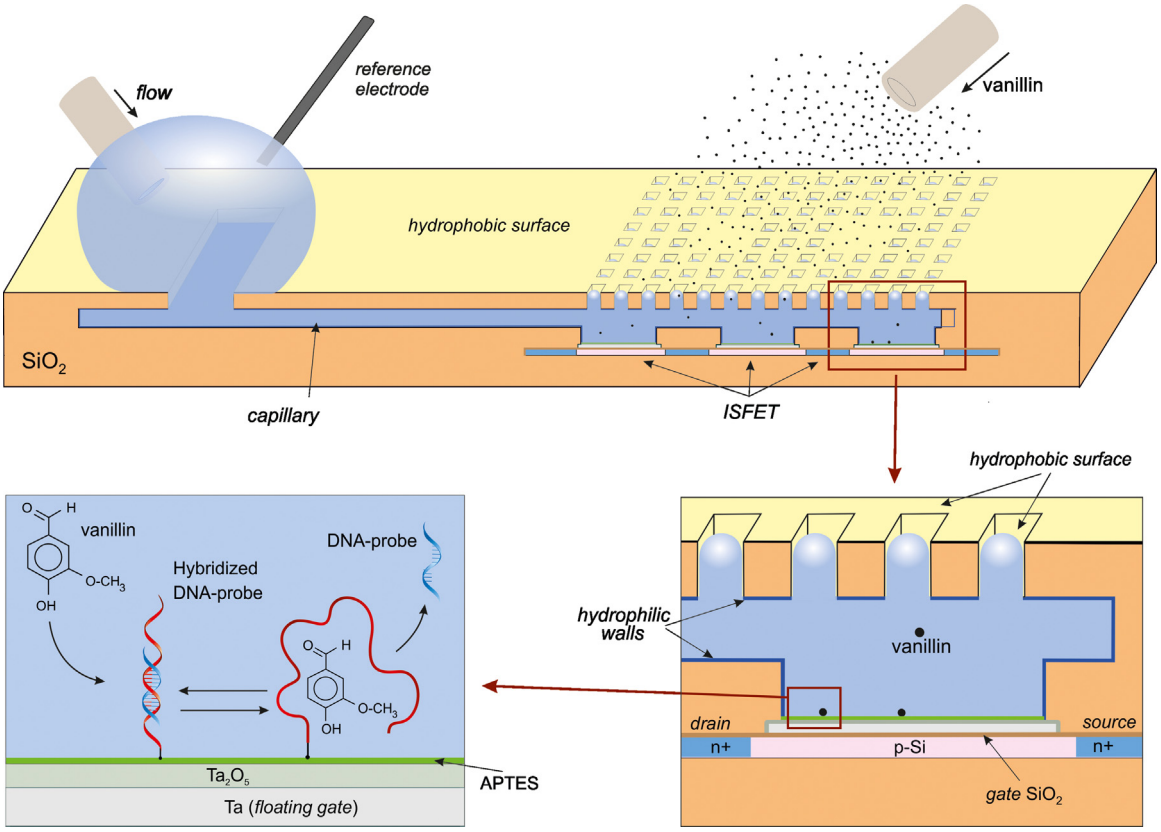

Fig. 1. General scheme of the developed bioelectronic element.

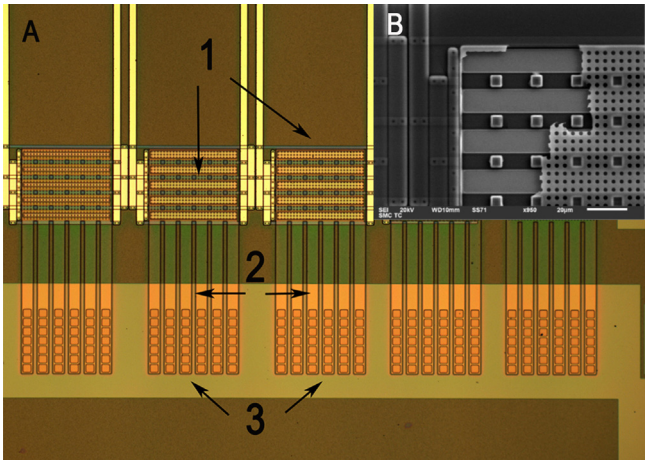

Fig. 2. A) Photo of the developed bioelectronic element: 1 – ISFETs under membrane, 2 – capillary microchannels, 3 – access ports; B) REM photo of the developed bioelectronic element (membrane was locally broken for the image).

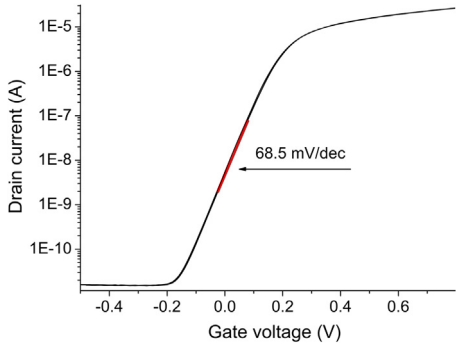

Fig. 3. Current-voltage characteristics of developed ISFETs.

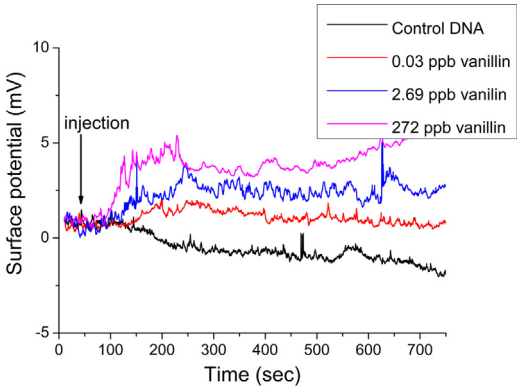

Fig. 4. Real time signal of the modified ISFETs after vanillin addition.

increase during DNA probe dehybridization. The utilized scheme allows for overcoming the limitation of ISFET:low sensitivity to direct detection of the interaction between small molecule and immobilized DNA.

The biosensor was tested regarding DNA dehybridization reaction by injection of 1 mL of gas samples collected from sealed test tubes. Test tubes contained 100 µL of vanillin with concentrations ranging from 6.5×10^{-7} M to 6.5×10^{-2} M and heated at 80 °C for vanillin evaporation.

The surface potential of the ISFET with Van74 started to increase approximately 30–40 s after vanillin addition. Conversely, the surface potential of ISFET with control DNA (nonfunctional DNA hybridized with the same probe) did not change significantly after vanillin

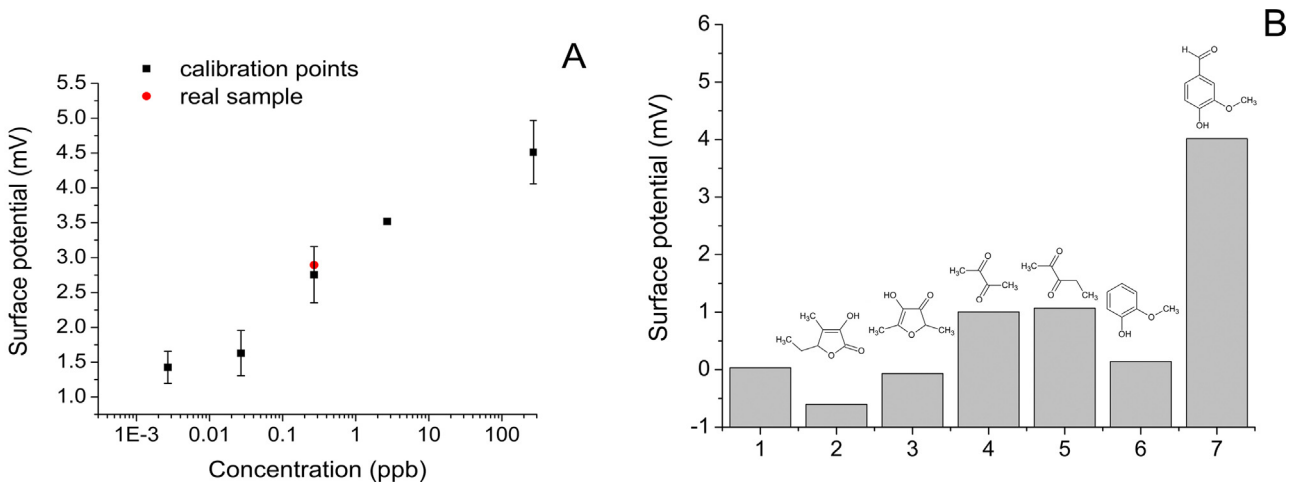

Fig. 5. A) Calibration curve for the sensor with estimation of real sample; B) Cross-selectivity of the developed sensor: 1 - steam, 2 - maple furanone, 3 - furaneol, 4-2,3-butanedione, 5-2,3-pentanedione, 6 – guaiacol, 7 – vanillin. The concentration of odour compounds was the same for all samples: 100 μL of 50 mM compound solutions were placed in 15 mL tubes, heated for 1 h at 80 °C, and then a probe of 1 mL of air from each tube was used as a sample.

injection (Fig. 4).

The intensity of the response showed a concentration-dependent increase as the concentration of vanillin increased (Fig. 5A). The calibration curve for vanillin determination showed that vanillin can be detected over a concentration range from 2.7 ppt to 0.3 ppm. The limit of detection (LOD) for vanillin was estimated to be 2.7 ppt. These results indicate that the gaseous vanillin molecules penetrate through the hydrophobic membrane and bind with aptamers immobilized on the bottom of the microfluidic chamber.

To verify the selectivity of the proposed sensor, we investigated the sensor response to injection of odour molecules that are present in roasted robusta coffee beans: guaiacol, 2,3-pentanedione, 2,3-butanedione, furaneol and maple furanone (Czerny et al., 1999; Blank et al., 1991). Prior to this, we found that the sensor did not respond to steam addition. Addition of guaiacol generated a small response comparable to baseline noise. This result is in good agreement with our previous results, in which we have shown that Van74 has good cross-reactivity to structure analogues (Kuznetsov et al., 2018). Addition of furanones led to a small decrease of surface potential value, and 2,3-pentanedione and 2,3-butanedione provided similar signal increases to 1 mV (Fig. 5B). The response generated by the gaseous vanillin was much stronger than that generated by the other odourant molecules, indicating that the sensor can discriminate between vanillin and other molecules presented in coffee aroma.

Finally, to demonstrate the ability of our bioelectronic nose to detect vanillin selectively in a complex matrix, we prepared genuine samples from green coffee with addition of vanillin. The added vanillin was successfully detected in the presence of the other odour molecules presented in roast beans (Fig. 5A).

Presented data demonstrate that Van74 immobilized under hydrophobic membrane possesses an ability to function appropriately and to mimic the olfactory receptor. It is worth mentioning that, in comparison to some olfactory receptors such as odourant binding proteins, the DNA aptamer may exhibit affinity in the same micromolar range (Pevsner et al., 1990). Using DNA aptamers for different targets, it becomes possible to design an array of ISFETs for odour discrimination. For example, an array of sensors where a single ISFET-based aptasensor selectively detects odour molecules presented in coffee aroma - such as guaiacol derivatives, aldehydes, furanones and some alkyl pyrazines - will enable identification of coffee origin (Czerny et al., 1999).

Comparison of different analysis techniques for odourants shows that the proposed approach has a number of significant advantages over existing systems (Table 1).

However, it should be mentioned that we had an issue during our work with low signal-to-noise ratio that limited signal processing in IC. This limitation may be overcome by increasing functional DNA aptamer density on the sensitive surface by optimized immobilization, developing new sensor design or selecting aptamers with higher affinity to target molecules. Another way to increase signal-to-noise ratio is to use a chemical amplification mimicking cascade reaction within the cell in the manner we demonstrated previously (Andrianova et al., 2018). Despite this limitation, the concept of bioelectronic nose presented here offers enormous potential. First, developed fabrication techniques are fully compatible with standard CMOS technology without additional post-processing steps, which enables the use of existing semiconductor factories and reduces production costs. Moreover, CMOS technology allows integrating an array of ISFET sensors with data processing on a single chip. Furthermore, due to advances in SELEX biotechnology, combination of ISFETs with aptamer arrays represents a flexible system setup configurable for different odours. This can find practical application in the fields of quality control of food products and perfumes, medical diagnosis and detection of hazardous substances.

4. Conclusions

A novel concept for bioelectronic nose application based on an aptamer-modified ISFET integrated with gas-liquid interface was developed. The construction of the system includes the ISFET as immersed under the hydrophobic membrane in the hydrophilic chamber with capillaries on the silicon chip. Hydrophilicity and hydrophobicity of capillary walls is engendered by silanes with different functional groups, wherein the sensitive surface remains free for further aptamer immobilization. Target molecules of vanillin penetrate through the hydrophobic membrane and interact with immobilized aptamer Van74 by the release of hybridized probe. The developed sensor was capable of detecting vanillin at a concentration as low as 2.7 ppt with excellent selectivity against the background of other odourant molecules presented in the odour of roasted coffee beans. These results demonstrate that the developed sensor can be used for the rapid and simple determination of odourant molecules in a complex matrix. Application of aptamers for different targets results in a flexible system setup configurable for different odours. Further work will be aimed at increasing the signal-to-noise ratio of the suggested system.

Table 1
Comparison of different analysis techniques for odourants.

Methods	Advantages	Disadvantages
GS/MS methods	Single species determination	Special sample preparation
	High sensitivity	High cost
	High selectivity	Trained personnel
		Long analysis time
Electronic noses	Low cost of analysis	The inability to determine the concentration of an individual compound
	No sample preparation required	
	Fact analysis	Low selectivity
	Continuous measurement	Dependence on humidity and temperature
	Portability and autonomy	Need for integration with different signal processing systems
Bioelectronic noses	Single species determination	Pre-extraction is required from the gas phase
	High selectivity	Low biomaterial stability
	Portability	The high cost of bioreceptors
	Fast analysis	Long cycle of the development of bioreceptors for new compounds
In this work	Single species determination	Low signal-to-noise ratio
	Portability	Complicated technology
	No sample preparation and extraction required	
	The relative stability of the biomaterial	
	The ability to quickly obtain receptors for new compounds	
	The low cost of aptamers	
	The ability to create a matrix of sensors with integrated signal processing on a single chip	

CRediT authorship contribution statement

Alexander E. Kuznetsov: Conceptualization, Formal analysis, Writing - original draft, Writing - review & editing, Supervision, Investigation. **Natalia V. Komarova:** Investigation, Writing - review & editing, Formal analysis. **Evgeniy V. Kuznetsov:** Conceptualization, Methodology, Formal analysis, Software, Visualization. **Maria S. Andrianova:** Investigation, Writing - review & editing, Visualization, Formal analysis, Validation. **Vitaliy P. Grudtsov:** Investigation, Validation. **Elena N. Rybachek:** Investigation, Resources. **Kirill V. Puchnin:** Investigation, Resources. **Dmitriy V. Ryazantsev:** Software, Investigation, Formal analysis. **Alexander N. Saurov:** Project administration, Funding acquisition, Supervision.

Acknowledgements

This work was supported by the Russian Science Foundation (project #16-19-10697). We thank the Center of Collective Use “Functional Control and Diagnostics of Micro- and Nanosystem Engineering based on R&D Technological Center” (Moscow, Zelenograd) for allowing access to their equipment.

Conflicts of interest

There are no conflicts to declare.

Appendix A. Supporting information

Supplementary data associated with this article can be found in the online version at doi:10.1016/j.bios.2019.01.013.

References

Andrianova, M.S., Gubanova, O.V., Komarova, N.V., Kuznetsov, E.V., Kuznetsov, A.E., 2016. Development of a biosensor based on phosphotriesterase and n-channel ISFET for detection of pesticides. Electroanalysis 28 (6), 1311–1321.
Andrianova, M., Komarova, N., Grudtsov, V., Kuznetsov, E., Kuznetsov, A., 2018. Amplified detection of the aptamer-vanillin complex with the use of Bsm DNA polymerase. Sensors 18, 49.
Blank, I., Sen, A., Grosch, W., 1991. Aroma Impact Compounds of Arabica and Robusta Coffee. Qualitative and Quantitative Investigations. In 14th International Scientific Colloquium on Coffee, San Francisco. ASIC, Paris, pp. 117–129.
Carl, L. Yaws, 2015. TheYaws Handbook of Vapor Pressure, 2nd ed. Gulf Professional Publishing.
Cave, J.W., Kenneth, J., Mitropoulos, A.N., 2019. Progress in the development of olfactory-based bioelectronic chemosensors. Biosens. Bioelectron. 123, 211–222.
Czerny, M., Mayer, F., Grosch, W., 1999. Sensory study on the character impact odorants of roasted Arabica coffee. J. Agric. Food Chem. 47, 695–699.
Di Pietrantonio, F., Cannatà, D., Benetti, M., Verona, E., Varriale, A., Staiano, M., D'Auria, S., 2013. Detection of odorant molecules via surface acoustic wave biosensor array based on odorant-binding proteins. Biosens. Bioelectron. 41, 328–334.
Elbaz, J., Shlyahovsky, B., Li, D., Willner, I., 2008. Parallel analysis of two analytes in solutions or on surfaces by using a bifunctional aptamer: applications for biosensing and logic gate operations. ChemBioChem 9 (2), 232–239.
Ellington, A.D., Szostak, J.W., 1990. In vitro selection of RNA molecules that bind specific ligands. Nature 346, 818–822.
Fitzgerald, J., Fenniri, H., 2017. Cutting edge methods for non-invasive disease diagnosis using e-tongue and e-nose devices. Biosensors 7, 59.
Goldsmith, B.R., Mitala, J.J., Josue, J., Castro, A., Lerner, M.B., Bayburt, T.H., Khamis, S.M., Jones, R.A., Brand, J.G., Sligar, S.G., Luetje, C.W., Gelperin, A., Rhodes, P.A., Discher, B.M., Johnson, A.T.C., 2011. Biomimetic chemical sensors using nanoelectronic readout of olfactory receptor proteins. ACS Nano 5, 5408–5416.
Göpel, W., 2000. From electronic to bioelectronic olfaction, or: from artificial “moses” to real noses. Sens. Actuators B Chem. 65, 70–72.
Hou, Y., Jaffrezic-Renault, N., Martelet, C., Tlili, C., Zhang, A., Pernollet, J.-C., Briand, L., Gomila, G., Errachid, A., Samitier, J., Salvagnac, L., Torbiéro, B., Temple-Boyer, P., 2005. Study of langmuir and langmuir−blodgett films of odorant-binding protein/amphiphile for odorant biosensors. Langmuir 21, 4058–4065.
Khosravi, A., Vossoughi, M., Shahrokhian, S., Alemzadeh, I., 2012. Nano reengineering of horseradish peroxidase with dendritic macromolecules for stability enhancement. Enzyme Microb. Technol. 50, 10–16.
Kuznetsov, A., Komarova, N., Andrianova, M., Grudtsov, V., Kuznetsov, E., 2018. Aptamer based vanillin sensor using an ion-sensitive field-effect transistor. Microchim. Acta 185 (3).
Lim, J.H., Park, J., Ahn, J.H., Jin, H.J., Hong, S., Park, T.H., 2013. A peptide receptor-based bioelectronic nose for the real-time determination of seafood quality. Biosens. Bioelectron. 39, 244–249.
Liu, Q., Cai, H., Xu, Y., Li, Y., Li, R., Wang, P., 2006. Olfactory cell-based biosensor: a first step towards a neurochip of bioelectronic nose. Biosens. Bioelectron. 22, 318–322.
Liu, Q., Ye, W., Hu, N., Cai, H., Yu, H., Wang, P., 2010. Olfactory receptor cells respond to odors in a tissue and semiconductor hybrid neuron chip. Biosens. Bioelectron. 26, 1672–1678.
Misawa, N., Mitsuno, H., Kanzaki, R., Takeuchi, S., 2010. Highly sensitive and selective odorant sensor using living cells expressing insect olfactory receptors. Proc. Natl. Acad. Sci. USA 107, 15340–15344.
Pevsner, J., Hou, V., Snowman, A.M., Snyder, S.H., 1990. Odorant-binding protein. characterization of ligand binding. J. Biol. Chem. 265 (11), 6118–6125.
Ruslinda, A.R., Tajima, S., Ishii, Y., Ishiyama, Y., Edgington, R., Kawarada, H., 2010. Aptamer-based biosensor for sensitive PDGF detection using diamond transistor. Biosens. Bioelectron. 26 (4), 1599–1604.
Sanaeifar, A., ZakiDizaji, H., Jafari, A., Guardia, M. de la, 2017. Early detection of contamination and defect in foodstuffs by electronic nose: a review. TrAC Trends Anal. Chem. 97, 257–271.
Schild, D., Restrepo, D., 1998. Transduction mechanisms in vertebrate olfactory receptor cells. Physiol. Rev. 78, 429–466.
Sharon, E., Freeman, R., Tel-Vered, R., Willner, I., 2009. Impedimetric or ion-sensitive field-effect transistor (ISFET) aptasensors based on the self-assembly of Au nanoparticle-functionalized supramolecular aptamer nanostructures. Electroanalysis 21 (11), 1291–1296.

So, H.M., Won, K., Kim, Y.H., Kim, B.K., Ryu, B.H., Na, P.S., Kim, H., Lee, J.O., 2005. Single-walled carbon nanotube biosensors using aptamers as molecular recognition elements. J. Am. Chem. Soc. 127 (34), 11906–11907.
Sung, J.H., Ko, H.J., Park, T.H., 2006. Piezoelectric biosensor using olfactory receptor protein expressed in Escherichia coli. Biosens. Bioelectron. 21, 1981–1986.
Tuerk, C., Gold, L., 1990. Systematic evolution of ligands by exponential enrichment: RNA ligands to bacteriophage T4 DNA polymerase. Science 249, 505–510.
Vidic, J.M., Grosclaude, J., Persuy, M.-A., Aioun, J., Salesse, R., Pajot-Augy, E., 2006. Quantitative assessment of olfactory receptors activity in immobilized nanosomes: a novel concept for bioelectronic nose. Lab Chip 6, 1026.
Wasilewski, T., Gębicki, J., Kamysz, W., 2017. Bioelectronic nose: current status and perspectives. Biosens. Bioelectron. 87, 480–494.
Wasilewski, T., Gębicki, J., Kamysz, W., 2018. Advances in olfaction-inspired biomaterials applied to bioelectronic noses. Sens. Actuators B Chem. 257, 511–537.
Westberg, D., Paul, O., Andersson, G.I., Baltes, H., 1996. Surface micromachining by sacrificial aluminium etching. J. Micromech. Microeng. 6, 376–384.
Wu, T.-Z., 1999. A piezoelectric biosensor as an olfactory receptor for odour detection: electronic nose. Biosens. Bioelectron. 14, 9–18.
Zayats, M., Huang, Y., Gill, R., Ma, C.A., Willner, I., 2006. Label-free and reagentless aptamer-based sensors for small molecules. J. Am. Chem. Soc. 128 (42), 13666–13667.